



# ACE2 Peptide Fragment Interaction with Different S1 Protein Sites

Aleksei Kuznetsov<sup>1</sup> · Piret Arukuusk<sup>2</sup> · Heleri Härk<sup>2</sup> · Erkki Juronen<sup>3</sup> · Mart Ustav<sup>2,3</sup> · Ülo Langel<sup>2,4</sup> · Jaak Järv<sup>1</sup>

Accepted: 21 November 2021 / Published online: 1 December 2021  
© The Author(s), under exclusive licence to Springer Nature B.V. 2021

## Abstract

We study the effect of the peptide QAKTFLDKFNHEAEDLFYQ on the kinetics of the SARS-CoV-2 spike protein S1 binding to angiotensin-converting enzyme 2 (ACE2), with the aim to characterize the interaction mechanism of the SARS-CoV2 virus with its host cell. This peptide corresponds to the sequence 24–42 of the ACE2  $\alpha$ 1 domain, which marks the binding site for the S1 protein. The kinetics of S1-ACE2 complex formation was measured in the presence of various concentrations of the peptide using bio-layer interferometry. Formation of the S1-ACE2 complex was inhibited by the peptide in cases where it was preincubated with S1 protein before the binding experiment. The kinetic analysis of S1-ACE2 complex dissociation revealed that preincubation stabilized this complex, and this effect was dependent on the peptide concentration as well as the preincubation time. The results point to the formation of the ternary complex of S1 with ACE2 and the peptide. This is possible in the presence of another binding site for the S1 protein beside the receptor-binding domain for ACE2, which binds the peptide QAKTFLDKFNHEAEDLFYQ. Therefore, we conducted computational mapping of the S1 protein surface, revealing two additional binding sites located at some distance from the main receptor-binding domain on S1. We suggest the possibility to predict and test the short protein derived peptides for development of novel strategies in inhibiting virus infections.

**Keywords** Peptide · Bio-layer interferometry · Peptide binding kinetics · SARS-CoV-2 spike protein · ACE2 peptide fragment · Allosteric binding site · Peptide docking

## Introduction

The binding of SARS-CoV-2 spike protein to the angiotensin-converting enzyme 2 (ACE2) on host cells leads to the fusion of virus and host cell membranes and initiates the entrance of viral RNA into the cells (Shang et al 2020; Song et al. 2018). The spike protein includes S1 and S2 domains, where S1 contains the receptor-binding domain (RBD) that binds to ACE2 (Wang et al 2020; Yan et al 2020). Reports suggest that blocking this binding step inhibits the virus entry process and thus may have therapeutic antiviral effects (Wu et al 2020). Because the molecular structure

of the S1-ACE2 complex is known (Wang et al 2020; Yan et al 2020; Lan et al 2020), and the atomic coordinates and experimental data have been deposited in the PDB database (code 6LZG, [www.wwpdb.org](http://www.wwpdb.org)), the most straightforward approach to design inhibitors of this binding process is to mimic the interaction interface between the spike protein and ACE2 molecule in this complex. As ACE2 is a physiologically important enzyme, its inhibition by antiviral prophylaxis with peptides derived from the spike protein is not a promising approach. Therefore, we focused on peptides derived from the ACE2 structure and interacting with the RBD of the spike protein S1.

Initially, the feasibility and viability of this approach was demonstrated in April 2020 by Han and Král (2020), who modelled binding of sequential  $\alpha$ -helices of the N-terminal part of ACE2 molecule with S1 receptor binding domain. These calculations revealed that binding energy of the  $\alpha_1$  peptide alone, containing amino acids 21–55 of the ACE2 sequence, was comparable with binding effectiveness of the  $\alpha_{1,2}$  sequence, and moreover with binding effectiveness of the whole ACE2 protein. Few weeks later (May 2020) Basit

✉ Jaak Järv  
jaak.jarv@ut.ee

<sup>1</sup> Institute of Chemistry, University of Tartu, Tartu, Estonia

<sup>2</sup> Institute of Technology, University of Tartu, Tartu, Estonia

<sup>3</sup> Icosagen Cell Factory OÜ, Tartu, Estonia

<sup>4</sup> Department of Biochemistry and Biophysics, Stockholm University, Stockholm, Sweden

et al (2021) confirmed this result, demonstrating that truncated ACE2 sequence, containing amino acids 21–119, is a potent binder to SARS-CoV-2 spike protein. Following these publications, results of systematic mapping of ACE2 binding site on the virus S1 protein were published by Kuznetsov and Järv (2020a) in June 2020. In this study it was shown that the peptide sequence, containing amino acids 19–45 of the  $\alpha$ 1 domain of the N-terminal part of ACE2, could be truncated from both ends without loss of binding effectiveness until the sequence 24–42 (QAKTFLDKFNHEAEDLFYQ) is reached. Thus, this peptide derived from the N-terminal part of ACE2, can be considered as the “minimal sequence”, needed for ACE2 recognition by the receptor binding domain (RBD) on the S1 protein of SARS-CoV-2 virus.

It is noteworthy that this conclusion has been confirmed by many following papers, which number exceeds 20 as of October 2021. All these works were also dealing with *in silico* peptide modelling and screening of their binding with the RBD of the spike protein. In addition, the specificity pattern of this interaction was specified (Kuznetsov and Järv 2020b) and the structural basis of the molecular recognition mechanism of these peptides was described (Freitas et al 2021). However, there is still no experimental data characterizing kinetics of interaction of these peptide fragments with the RBD on SARS-CoV-2 spike protein. In this paper we fill this gap by investigating kinetic aspects of the influence of the minimal peptide sequence QAKTFLDKFNHEAEDLFYQ on interaction of ACE2 and S1 protein, using bio-layer interferometry (BLI) (Frenzel and Willbold 2014).

As the molecular mass of the peptide QAKTFLDKFNHEAEDLFYQ is too low for a direct binding assay using bio-layer interferometry (BLI) (Frenzel and Willbold 2014), and it is unclear how chemical modification or loading of the peptide with a linker group (for example biotine) or cargo molecule would influence its binding properties, effect of the peptide on the kinetics of the S1-ACE2 interaction was studied. In these experiments ACE2 was loaded onto the biosensor surface and kinetics of S1 binding was monitored in the presence and absence of the minimal peptide QAKTFLDKFNHEAEDLFYQ. This kinetic approach is the only solid method to establish different types of complexes formed between this peptide and interacting proteins.

## Materials and Methods

### Peptide Synthesis

The peptide QAKTFLDKFNHEAEDLFYQ was synthesized on an automated peptide synthesizer (Biotage Initiator + Alstra, Sweden) using the fluorenylmethoxycarbonyl (Fmoc) solid-phase peptide synthesis strategy and

Rink-amide ChemMatrix resin (PCAS- BioMatrix, Québec, Canada) to obtain a C-terminally amidated product. *N,N'*-diisopropylcarbodiimide (DIC) and Oxyma Pure in dimethylformamide (DMF) were used as coupling reagents, and *N,N*-diisopropylethylamine (DIEA) was used as the activator base. Cleavage of the product was performed with trifluoroacetic acid (TFA), 2.5% triisopropylsilane (TIPS), and 2.5% water for three hours at room temperature.

The peptide was purified by high-performance liquid chromatography (HPLC) on a C4 column (Phenomenex Jupiter C4, 5  $\mu$ m, 300 Å, 250  $\times$  10 mm, Agilent) using an acetonitrile/water gradient containing 0.1% TFA. The purity of the peptide was validated at 98% using a Waters Acquity Ultra-Performance Liquid Chromatography (UPLC) with an acetonitrile/water gradient (Supplement Fig. S1). The accurate molecular weight of the peptide was determined to be 2342 Da using a matrix-assisted laser desorption/ionization time-of-flight (MALDI-TOF) mass spectrometer (Bruker Microflex LT/ SH, USA), with  $\alpha$ -cyano-4-hydroxycinnamic acid as the matrix (Supplement Fig S2). The calculated molecular weight of the peptide was 2342.15 Da.

### Proteins

Human recombinant ACE2-His protein (Icosagen OÜ, Estonia, cat# P-302–100) and SARS-CoV-2 Wuhan type spike protein S1 (Icosagen OÜ, Estonia, cat# P-305–100) were used in this study.

### Bio-Layer Interferometry (BLI)

His-tagged ACE2 was immobilized onto Octet RED96e biosensors (ForteBio, CA, USA), and the binding of S1 protein was measured in the presence and absence of peptide QAKTFLDKFNHEAEDLFYQ. Experiments were performed at 25 °C in 20 mM Tris–HCl pH 7.0 and 150 mM NaCl. Biosensors (HIS1K, lot 6,110,102) were loaded with His-tagged ACE2, prior to the addition of S1 protein only or S1 protein and peptide to initiate the complex formation process. In one series of experiments, the peptide was preincubated with S1 for 15 min at 25 °C before the binding assay. Complex dissociation was initiated by immersing the biosensors into fresh assay buffer (20 mM Tris–HCl pH 7.0 with 150 mM NaCl), without the S1 protein and peptide. Data were analyzed using the ForteBio Data Analysis software (version 11.1.1.39) (Tobias and Kumaraswamy, 2011). Results of the kinetic experiments are presented in the Supplement Tables S1–S4.

### Computational Peptide Docking

The peptide docking investigation was performed as described in previous studies (Kuznetsov and Jarv 2020a,

2020b). Briefly, the input file for modeling the S1-ACE2 complex was built from X-ray analysis data (Wang et al 2020; Lan et al 2020), deposited in the PDB database ([www.wwpdb.org](http://www.wwpdb.org)) with the code 6LZG. The GROMACS package (version 4.6.1) was used for molecular dynamics simulations (Hess et al 2008), and AutoDock Vina (version 1.1.2) was used for ligand docking (Trott and Olson 2010). The best scores were selected for peptide positioning. Protein protonation at pH 7 was processed using the GROMACS pdb2gmx tool, and the geometric, charge, and van der Waals constrained parameters were assigned using the GROMOS 53a6 force field parameter set (Oostenbrink et al 2004). The protein structure, neutralized by adding  $\text{Na}^+$  and  $\text{Cl}^-$  ions, was solvated in a 5 nm cubic box, filled with SPC water as solvent (Berendsen and Grigera 1987). The system was allowed to reach equilibrium at constant pressure 1 atm (Parrinello and Rahman 1981) and temperature (300 K) was controlled by the modified Berendsen thermostat algorithm (Berendsen et al 1984). Equilibrated simulations were performed on the systems for ten nanoseconds. After MD relaxation, the protein structure was extracted from the system and used for docking procedures. The docking compatible structure formats of the protein were prepared by AutoDockTools, version 1.5.6 (Morris et al 2009). The fitting box with 0.3 Å grid spacing was defined once and used for all docking calculations. The fitting area covered the whole protein space, and the docking poses were obtained and listed according to the docking energy values. The graphic software package VMD (version 1.9.4) was used to illustrate ligand docking poses on the protein surface (Humphrey et al 1996).

## Results and Discussion

### Kinetic Measurements of S1-ACE2 Interaction

The effect of the peptide QAKTFLDKFNHEAEDLFYQ on binding of SARS-CoV-2 spike S1 protein with ACE2 was investigated by loading ACE2 onto a biosensor, and dipping this sensor into a buffer containing S1 protein, or S1 protein and peptide. This experimental setup allowed characterization of the complex formation and dissociation reactions, described by the ascending and descending parts of the graphs, respectively, as shown in Fig. 1. According to the ascending part of the plot, the complex formation reaction is characterized by the first-order rate constant  $k_{\text{on}}$  ( $\text{s}^{-1}$ ) and the second-order rate constant  $k_{\text{ass}}$  ( $\text{M}^{-1} \text{s}^{-1}$ ). The concentration of the S1 protein in the assay buffer should be taken into consideration for calculation of the latter parameter (Frenzel and Willbold 2014). The descending part of the plot allows calculation of the complex dissociation rate constant, denoted by  $k_{\text{off}}$  ( $\text{s}^{-1}$ ). The equilibrium constant for the

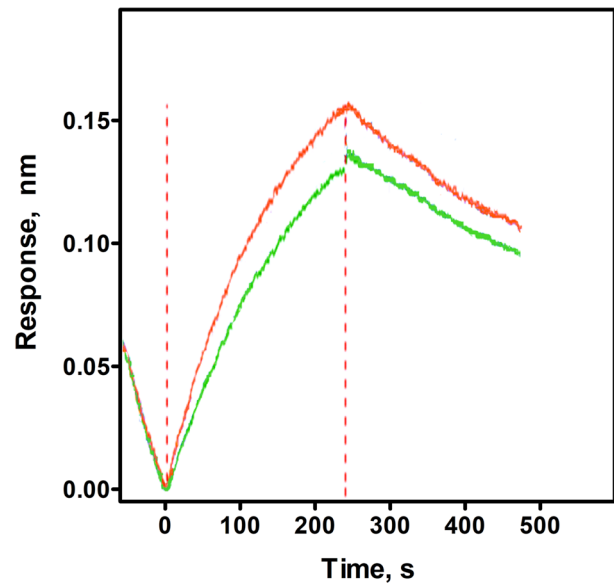


**Fig. 1** Kinetic curves characterizing the time course of SARS-CoV-2 spike protein S1 binding to ACE2 protein loaded onto biosensors (ascending curve) and dissociation of this complex (descending curve). Red line: experiment performed using the assay buffer without the peptide. Green line: experiment performed in the presence of 5  $\mu\text{M}$  peptide QAKTFLDKFNHEAEDLFYQ, preincubated with the SARS-CoV-2 spike protein S1 for 15 min

complex dissociation,  $K_D$ , is calculated as the ratio between the  $k_{\text{off}}$  and  $k_{\text{ass}}$  values (Frenzel and Willbold 2014; Tobias and Kumaraswamy 2014).

In this study, the  $K_D$  values for the S1-ACE2 complex dissociation, calculated from parallel experiments in the absence of the peptide, were  $(1.28 \pm 0.01) \times 10^{-8} \text{ M}$ ,  $(3.05 \pm 0.01) \times 10^{-8} \text{ M}$  and  $(7.76 \pm 0.10) \times 10^{-8} \text{ M}$ , respectively (Tables S1, S2 and S3 in the Supplement). These values agree with the  $K_D = 2.9 \times 10^{-8} \text{ M}$ , published by Reaction Biology (Hewitt 2021), and confirm the reliability of the assay procedure.

### Peptide Effect on S1 and ACE2 Interaction Kinetics

Figure 1 shows that the time course of interaction of the spike protein S1 with ACE2 (red line) is affected by the addition of 5  $\mu\text{M}$  peptide (green line). For a more detailed analysis of this effect, two series of kinetic experiments were performed, in which different amounts of the peptide was added to the kinetic assay. In the first series, the S1 protein and the peptide were added simultaneously to the sensor-immobilized ACE2 to initiate the complex formation. In the second series of experiments, S1 protein was preincubated with the peptide during 15 min before addition to the sensor-immobilized ACE2. In both cases the  $k_{\text{on}}$  values were determined (Tables S1 and S2 in the Supplementary Section), and the relative values  $k_{\text{on}}^{\text{rel}}$  were calculated as ratio of the

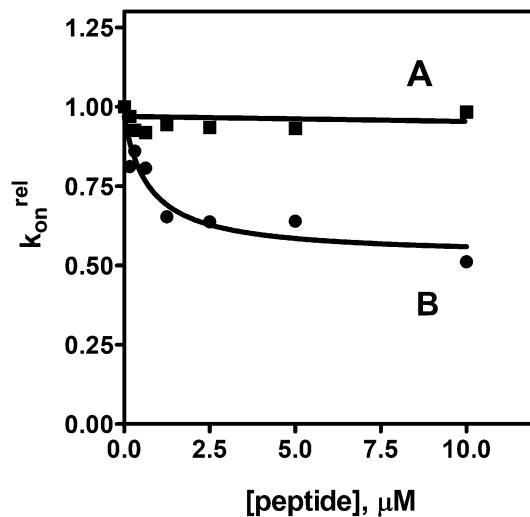


**Fig. 2** Effect of peptide QAKTFLDKFNHEAEDLFYQ on the rate constant of S1 binding with ACE2, immobilized on the biosensor ( $k_{\text{on}}$ ). A. Spike protein S1 and peptide were simultaneously added into the assay buffer to initiate the binding reaction of S1 with ACE2 (squares). B. Preincubation of spike protein S1 with peptide was made during 15 min before the binding reaction of S1 with ACE2 was initiated (circles)

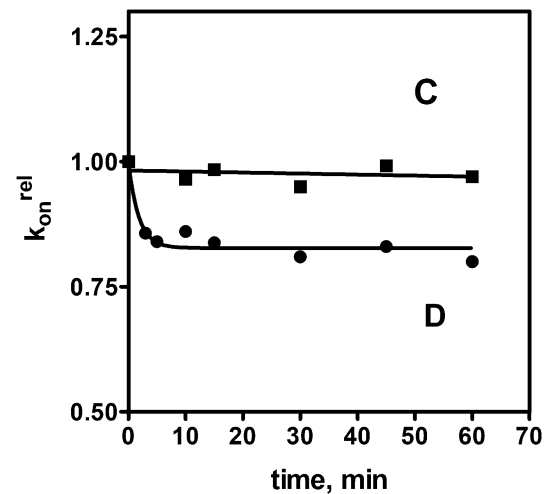
rate constants measured in the absence and in the presence of the peptide. The results of these experiments are summarized in Fig. 2.

Figure 2 shows that the peptide QAKTFLDKFNHEAEDLFYQ has no effect on rate of the S1-ACE2 complex formation, when S1 and the peptide were added simultaneously into the assay buffer (Series A). In contrast, however, the rate of the complex formation was inhibited when S1 protein was preincubated with the peptide (15 min) before the complex formation reaction was started (Series B). Consequently, some time is needed to load the S1 protein with the peptide before binding with ACE2 to see the inhibitory effect, and this loading seems to be a relatively slow process.

Secondly, Fig. 2 also shows that the peptide inhibits the complex formation reaction in dose-dependent manner, and the half-maximal inhibitory effect is reached at  $0.7 \pm 0.4 \mu\text{M}$  peptide concentration.

Thirdly, it can be seen that only partial inhibition of the complex formation reaction occurs in the presence of the peptide. This can be explained by formation of a ternary complex. In this case this ternary complex includes the peptide, S1 and ACE2.

The time course of S1 loading with the peptide was studied separately, using different preincubation times ranging from 3 to 60 min (Tables S3 and S4 in the Supplementary Information). The results of this analysis are summarized in Fig. 3. These data show that the half-life of the loading process is approx. 2 min at peptide concentration  $5 \mu\text{M}$ . On the other hand, however, the loading process is fast enough



**Fig. 3** Effect of preincubation time of peptide QAKTFLDKFNHEAEDLFYQ with S1 protein on the rate constant of S1 binding to ACE2 ( $k_{\text{on}}$ ), where ACE2 is immobilized on the biosensor. The spike protein S1 was preincubated in the assay buffer with no peptide (series C, squares), and with  $5 \mu\text{M}$  peptide (series D, circles), before the binding assay was initiated

to rule out the possibility that the above-described phenomenon of partial inhibition can be explained by slowness of the peptide interaction with S1 protein, and thus these kinetic data confirm the possibility of the formation of the ternary S1-peptide-ACE2 complex.

### Peptide Effect on S1-ACE2 Complex Dissociation Kinetics

Dissociation of the ACE2 bound S1 protein was initiated by transferring the biosensor-bound complex into fresh assay buffer that did not contain peptide or S1 protein, and the rate constants  $k_{\text{off}}$  were obtained (Tables S1 and S2 in the Supplementary Section). From these data the relative  $k_{\text{off}}$  values were calculated as described above, and plotted in Fig. 4.

It is important to mention that similar  $k_{\text{off}}$  values should characterize the dissociation process in all experiments, if similar binary complex is formed between the ACE2 and S1 protein on the sensor chip. However, this was not the case in this study. Figure 4 shows that preincubation of the S1 protein with the peptide has stabilized the complex, as all  $k_{\text{off}}^{\text{rel}}$  values in Series B (Table S2, Supplementary Information) were lower than the equivalent values in Series A (Table S1). Moreover, this plot was clearly dose-dependent, although no peptide was added into the assay medium in the off-rate experiment.

Secondly, the off-rate kinetic data, characterized by the  $k_{\text{off}}^{\text{rel}}$  values, also depend on the preincubation time of the S1 protein with the inhibitory peptide, as shown in Fig. 5. This time-course is characterized by half-life 14 min.

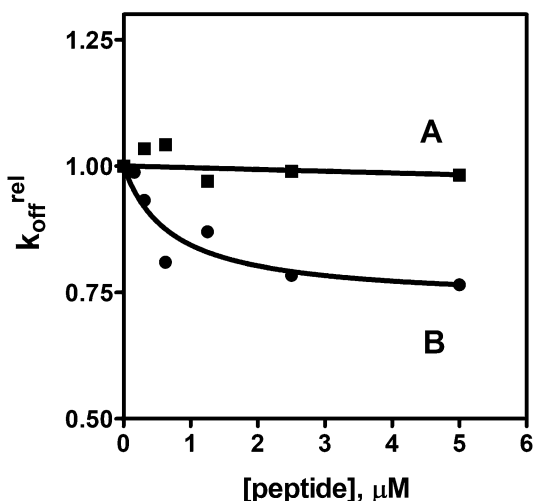


**Fig. 4** Dissociation of S1-ACE2 complex, captured by the biosensor in the binding assay. The S1-ACE2 protein complex was formed in the presence of different peptide concentrations in experiments where the S1 protein had not been preincubated with the peptide (series A, squares), or where the S1 protein had been preincubated with the peptide for 15 min (series B, circles). To initiate the dissociation process, the biosensor was transferred into fresh buffer that did not contain the peptide and S1 protein, and the peptide concentrations indicated are those used in the binding assay

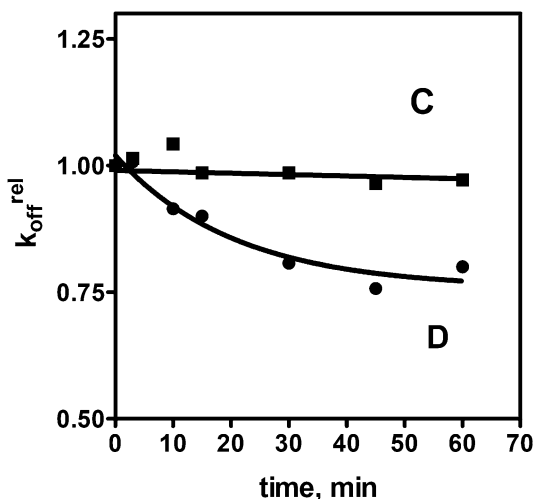


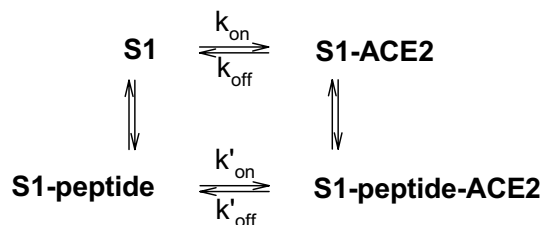
**Fig. 5** Effect of peptide QAKTFLDKFNHEAEDLFYQ preincubation time with S1 protein in the S1-ACE2 complex formation experiment (no peptide, series C; 5  $\mu M$  peptide, series D) on the dissociation rate ( $k_{off}$ ) of the same complex, immobilized on the biosensor soaked into buffer without added peptide

**Ternary Complex**

The occurrence of the observed “memory” of the S1–ACE2 complex about the presence of the peptide in the previous complex formation step indicates that the peptide has remained in the complex and therefore affects its stability.

From a chemistry point of view, this is possible if there is a separate binding site for this peptide on the S1 protein, as the conventional receptor-binding site (RBD) must be occupied by the  $\alpha 1$  domain of ACE2. Thus, the off-rate kinetic data confirm the presence of an alternative binding site or sites for the peptide and agree with the idea about the formation of the ternary complex S1-peptide-ACE2.

The putative reaction scheme that describes the influence of the preloading process of the S1 protein with the peptide and the consecutive binding of this complex with ACE2, is shown below.



It can be concluded that the inhibitory effect of the peptide is uncompetitive, as far as the equilibrium between the binary and tertiary complexes of ACE2 exists. This equilibrium also points to the possibility that at least two different binding sites exist on the S1 protein, which can be specifically recognized by the  $\alpha 1$  domain of ACE2 and by the peptide derived from this sequence of this receptor protein: one of these sites should be involved in interaction with the ACE2 protein and the second should be responsible for the peptide binding.

Although there are no other kinetic studies, which discuss the mechanism of S1 protein interaction with the receptor protein, the idea of sequential binding of several ACE2 molecules with the spike protein has been expressed previously in a cryoEM study, where a 1: 3 stoichiometry of the spike protein-ACE2 complex was suggested (Benton et al 2020). It was also shown that the formation of multimeric complexes assumes significant conformational changes of participating proteins. This is not surprising, as structural transitions seem to play an important role already in the binding process of peptide fragments to the S1 protein, as kinetics of this process is slow. Therefore, understanding of the physiological meaning of the putative additional binding sites seems to be challenging and may open novel perspectives for the development of peptide-based antiviral therapeutic agents SARS-CoV-2 infection.

**Computational Study of Alternative Peptide Binding Modes on S1 Protein**

The hypothesis that additional (allosteric) binding sites exist on the S1-ACE2 complex, and these sites may bind peptide

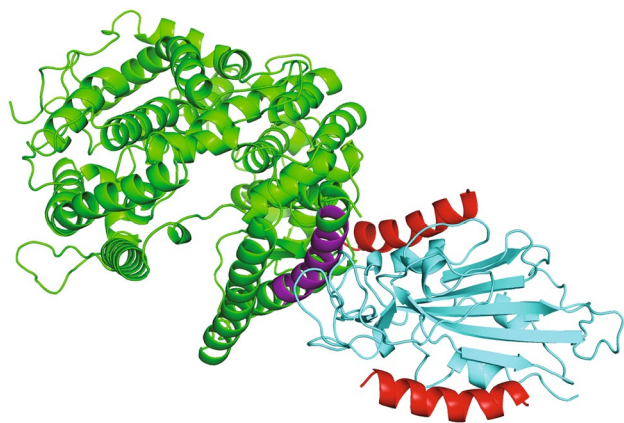


**Fig. 6** Computationally modeled ribbon structure of SARS-Cov-2 spike protein S1 and ACE2 complex. The S1 protein is shown in blue, while the ACE2 molecule is shown in green. Two allosterically bound peptide QAKTFLDKFNHEAEDLFYQ molecules are shown in red. The sequence (amino acids 24–42) of the  $\alpha 1$  domain of ACE2, interacting with the S1 protein, is shown in violet

molecules that cause the “memory” effect in the off-rate experiments, was investigated computationally by mapping the putative docking landscape outside the known ACE2 binding site on the S1 protein. These calculations reveal two allosteric binding possibilities for the peptide QAKTFLDKFNHEAEDLFYQ (Fig. 6).

The docking energies of the peptide at these alternative binding sites were  $E_{\text{dock}} = -10.7$  kcal/mol (upper location) and  $E_{\text{dock}} = -10.5$  kcal/mol (lower location), respectively, while the docking energy of the same peptide in the recognized receptor binding domain (RBD) of S1 was  $-11.6$  kcal/mol (violet) (Kuznetsov and Jarv 2020a). As these additional sites do not overlap with the RBD, peptide binding in these sites will not necessarily compete with S1 binding to ACE2; however, there may be an allosteric effect. Importantly, these allosteric sites are also available in the free S1 protein that explains the experimentally observed “memory” effect, where the influence of the peptide applied in the preincubation step is revealed in a dose-dependent manner in the complex off-rate kinetics.

## Conclusions

The peptide QAKTFLDKFNHEAEDLFYQ, defined as “minimal sequence” of ACE2 structure that selectively recognizes the CoV-2 virus S1 protein, interferes binding of the S1 protein with ACE2 in the model experiment. The kinetic mechanism of this interaction is complex, as uncompetitive inhibition of S1-ACE2 complex formation was observed after preloading of the S1 protein with the peptide. These

results point to possibility of multiple binding modes and the presence of different binding sites on S1 protein.

Furthermore, it is important to highlight that although the on-rate and off-rate of the S1-ACE2 complex formation process ( $k_{\text{on}}$  and  $k_{\text{off}}$ ) depend on the peptide concentration (Figs. 2, 4), there is practically no effect of this peptide on the  $K_d$  value, determined by the ratio of the same kinetic parameters. Thus, ligand interaction with the S1 protein may not shift the observed equilibrium of S1 binding to ACE2, but instead change its dynamics. This is an important concept to be considered in the design of antiviral therapeutics, as the equilibrium-based inhibition mechanism of drug binding, as commonly suggested, may be oversimplified.

**Supplementary Information** The online version contains supplementary material available at <https://doi.org/10.1007/s10989-021-10324-7>.

**Acknowledgements** Computational analysis was performed in the High-Performance Computing Center, and the peptide was synthesized in the Core Laboratory of Peptide Chemistry of the University of Tartu.

**Authors' Contributions** PA and HH performed peptide synthesis and analysis, EJ made kinetic experiments, AK performed computations and contributed to study conception. MU, ÜL and JJ planned this study, performed data analysis and interpretation. The first draft of the manuscript was written by JJ and all authors contributed to this work and commented on next versions of the manuscript.

**Funding** This work was financially supported by QanikDX OÜ (Estonia, Registration Number 4523084, Grant LLTLT20014).

**Data Availability** Experimental data are shown in Supplement Information to this paper.

## Declarations

**Conflict of interest** The authors declare no competing interests.

## References

- Basit A, Ali T, Rehman SU (2021) Truncated human angiotensin converting enzyme 2; a potential inhibitor of SARS-CoV-2 spike glycoprotein and potent COVID-19 therapeutic agent. *J Biomol Struct Dyn* 39:3605–3614. <https://doi.org/10.1080/07391102.2020.1768150>
- Benton DJ, Wrobel AG, Xu P, Roustan C, Martin SR, Rosenthal PB, Skehel JJ, Gamblin SJ (2020) Receptor binding and priming of the spike protein of SARS-CoV-2 for membrane fusion. *Nature* 588:327–330. <https://doi.org/10.1038/s41586-020-2772-0>
- Berendsen HJC, Postma JPM, van Gunsteren WF, DiNola A, Haak JR (1984) Molecular dynamics with coupling to an external bath. *J Chem Phys* 81:3684–3690. <https://doi.org/10.1063/1.448118>
- Berendsen HJC, Grigera JR, Straatsma TP (1987) The missing term in effective pair potentials. *J of Phys Chem* 91:6269–6271. <https://doi.org/10.1021/j100308a038>
- Freitas FC, Ferreira PHB, Favaro DC, Oliveira RJ (2021) Shedding light on the inhibitory mechanisms of SARS-CoV-1/CoV-2 spike proteins by ACE2-designed peptides. *J Chem Inf Model* 22:1226–1243. <https://doi.org/10.1021/acs.jcim.0c01320>

- Frenzel D, Willbold D (2014) Kinetic titration series with biolayer interferometry. *PLoS ONE* 9:e106882. <https://doi.org/10.1371/journal.pone.0106882>
- Han Y, Král P (2020) Computational design of ACE2-based peptide inhibitors of SARS-CoV-2. *ACS Nano* 14:5143–5147. <https://doi.org/10.1021/acsnano.0c02857>
- Hess B, Kutzner C, van der Spoel D, Lindahl E (2008) GROMACS 4: algorithms for highly efficient, load-balanced, and scalable molecular simulation. *J Chem Theory Comput* 4:435–447. <https://doi.org/10.1021/ct700301q>
- Hewitt J (2021) Biophysical characterization of compounds disrupting the SARS-CoV-2 Spike – ACE2 interaction. *Reaction Biology*. <https://www.reactionbiology.com/resources/reading-room/blog/biophysical-characterization-compounds-disrupting-sars-cov-2-spike-ace2>. Accessed 20 August 2021
- Humphrey W, Dalke A, Schulten K (1996) VMD: visual molecular dynamics. *J Mol Graph* 14:33–38. [https://doi.org/10.1016/0263-7855\(96\)00018-5](https://doi.org/10.1016/0263-7855(96)00018-5)
- Kuznetsov A, Järv J (2020a) Mapping of ACE2 binding site on SARS-CoV-2 spike protein S1: docking study with peptides. *Proc Est Acad Sci* 69:228–234. <https://doi.org/10.3176/proc.2020.3.06>
- Kuznetsov A, Järv J (2020b) Mapping the ACE2 binding site on the SARSCoV2 spike protein S1: molecular recognition pattern. *Proc Est Acad Sci* 69:355–360. <https://doi.org/10.3176/proc.2020.4.09>
- Lan J, Ge J, Yu J, Shan S, Zhou H, Fan S, Zhang Q, Shi X, Wang Q, Zhang L, Wang X (2020) Structure of the SARS-CoV-2 spike receptor-binding domain bound to the ACE2 receptor. *Nature* 581:215–220. <https://doi.org/10.1038/s41586-020-2180-5>
- Morris GM, Huey R, Lindstrom W, Sanner MF, Belew RK, Goodsell DS, Olson JA (2009) AutoDock4 and AutoDockTools4: automated docking with selective receptor flexibility. *J Comput Chem* 30:2785–2791. <https://doi.org/10.1002/jcc.21256>
- Oostenbrink C, Villa A, Mark AE, van Gunsteren WF (2004) A biomolecular force field based on the free enthalpy of hydration and solvation: the GROMOS force-field parameter sets 53A5 and 53A6. *J Comput Chem* 25:1656–1676. <https://doi.org/10.1002/jcc.20090>
- Parrinello M, Rahman A (1981) Polymorphic transitions in single crystals: a new molecular dynamics method. *J Appl Phys* 52:7182–7190. <https://doi.org/10.1063/1.328693>
- Shang J, Ye G, Shi K, Wan Y, Luo C, Aihara H, Geng Q, Auerbach A, Li F (2020) Structural basis of receptor recognition by SARS-CoV-2. *Nature* 581:221–224. <https://doi.org/10.1038/s41586-020-2179-y>
- Song W, Gui M, Wang X, Xiang Y (2018) Cryo-EM structure of the SARS coronavirus spike glycoprotein in complex with its host cell receptor ACE2. *PLoS Pathog*. <https://doi.org/10.1371/journal.ppat.1007236>
- Tobias R, Kumaraswamy S (2014) Biomolecular binding kinetics assays on the octet platform. *Forste Bio. Appl. Note* 14:1–21. <http://separations.co.za/wp-content/uploads/2017/05/OCTET.pdf> Accessed 19 August 2021
- Trott O, Olson JA (2010) AutoDock Vina: improving the speed and accuracy of docking with a new scoring function, efficient optimization, and multithreading. *J Comput Chem* 31:455–461. <https://doi.org/10.1002/jcc.21334>
- Wang Q, Zhang Y, Wu L, Niu S, Song C, Zhang Z, Lu G, Qiao C, Hu Y, Yuen KY, Wang Q, Zhou H, Yan J, Qi J (2020) Structural and functional basis of SARS-CoV-2 entry by using human ACE2. *Cell* 181:894–904. <https://doi.org/10.1016/j.cell.2020.03.045>
- Wu C, Liu Y, Yang Y, Zhang P, Zhong W, Wang Y, Wang Q, Xu Y, Li M, Li X, Zheng M, Chen L, Li H (2020) Analysis of therapeutic targets for SARS-CoV-2 and discovery of potential drugs by computational methods. *Acta Pharm Sin B* 10:766–788. <https://doi.org/10.1016/j.apsb.2020.02.008>
- Yan R, Zhang Y, Li Y, Xia L, Guo Y, Zhou Q (2020) Structural basis for the recognition of SARS-CoV-2 by full-length human ACE2. *Science* 367:1444–1448. <https://doi.org/10.1126/science.abb2762>

**Publisher's Note** Springer Nature remains neutral with regard to jurisdictional claims in published maps and institutional affiliations.